Multibody Syst Dyn (2017) 40:1–22
DOI 10.1007/s11044-016-9515-x

Kinematic state estimation for rigid-link multibody systems by means of nonlinear constraint equations

Ilaria Palomba[1] · Dario Richiedei[1] · Alberto Trevisani[1]

Received: 15 June 2015 / Accepted: 4 March 2016 / Published online: 23 March 2016

Abstract In the multibody field the design of state observers proves useful for several tasks, ranging from the synthesis of control schemes and fault detection strategies, to the identification of uncertain parameters. State observers are designed to obtain accurate estimates of unmeasurable or unmeasured variables. Their accuracy and performance depend on both the models used and the measurement sets. In multibody systems, if it is reasonable to neglect joint clearance and to assume that links are rigid, the estimates of kinematic variables (i.e. position, velocity and acceleration) can be carried out very effectively using kinematic models, i.e. models based on kinematic constraint nonlinear equations, which provide much less uncertain models than dynamic equations. Under the aforementioned assumptions, this paper proposes a general theory, valid for both open-chain and closed-chain multibody systems, to design observers based on nonlinear kinematic models. The concurrent use of kinematic models and nonlinear estimators is original in the multibody field and represents the chief contribution of the paper. The soundness of the proposed theory is proved through numerical and experimental tests on both open-chain and closed-chain multibody systems. Finally, a comparison is given between the kinematic estimations computed through two nonlinear observers (the extended Kalman filter, EKF, and the spherical simplex unscented Kalman filter, SS-UKF), in order to demonstrate the benefits of the SS-UKF in nonlinear estimation.

Keywords Nonlinear state observers · Kinematic estimation · Rigid-link multibody systems

1 Introduction

Not only is the knowledge of the actual state of multibody systems (MBSs) an essential requirement for assuring proper motion through advanced control schemes [1], but it is also

✉ D. Richiedei
dario.richiedei@unipd.it

[1] Department of Management and Engineering (DTG), Università di Padova, 36100 Vicenza, Italy

useful in the implementation of techniques for fault detection, virtual sensors and of strategies for the identification of uncertain parameters. Unfortunately, the direct measurement of all the state variables (positions and velocities) is frequently unfeasible for technical or economical reasons. Therefore, the availability of efficient and effective techniques for the estimation of state variables in MBSs is often necessary.

To this end, closed-loop state observers (estimators) [2] are typically employed. An observer reconstructs the missing state variables by means of a reliable system model and of measurements of both the system inputs and outputs. Such a fusion of system model and sensor measurements allows tackling very effectively a wide class of issues. On the one hand, the closed-loop architecture of a state observer provides a means to compensate for model parameter errors, due to, for example, bad calibration, modeling errors, unexpected parameter changes. On the other, the use of a model, albeit uncertain, allows filtering external noise and hence avoiding the considerable delay that causal low-pass filters would introduce.

In the multibody field, the design of state observers has been typically based on Kalman filters employing dynamic equations of motion, also whenever the estimated state variables are only kinematic quantities, such as position, speed or acceleration [3, 4]. Such dynamic models are inherently uncertain because they depend on several uncertain geometric and inertial parameters (such as link dimensions, joint positions, actual mass and moments of inertia values, positions of centers of mass) and on external inputs (such as friction, control and disturbance forces), which are sometimes unknown. All these uncertainties may seriously compromise the accuracy and the performance of observers, and affects their actual usefulness in practical applications.

Whenever the system links are rigid and joint clearance is negligible, improvement of the estimates of kinematic state variables can be achieved by only involving kinematic quantities and by employing kinematic models instead of dynamic models. Indeed, kinematic models are geometrical models, which depend on a lower number of parameters and variables compared to dynamic ones. Additionally, estimation through kinematic model can be employed effectively regardless of the knowledge of the external forces and of the presence of joint friction, which are often difficult to measure or to estimate. In contrast, dynamic models need accurate knowledge of such a phenomenon to operate properly. State observers based on kinematic models have already been proposed in the literature [5, 6] and are known as Kinematic Kalman Filters (KKFs). In its original definition, a KKF is a sensor-based estimator where the measurement set is used both as the output and the input to first-order differential equations representing the kinematic model of a system. To the best of the authors' knowledge, so far kinematic state observers have been employed just to perform simple encoder–accelerometer sensor fusion (without the use of kinematic constraints) in a single body system [6], or to perform end-effector sensing both in a planar two-link robot [6] and in an industrial open chain robot [7]. In [8], an observer based on kinematic models has instead been used for kinematic parameter estimation in rigid body systems.

Clearly, there still lacks a comprehensive theory for kinematic state estimation, capable of dealing with both open-chain and closed-chain MBSs, and explicitly addressing the problems arising from the nonlinearity of state estimation. In particular, with reference to the latter issue, in all the quoted references, nonlinear kinematic state estimation has been performed using the discrete Extended Kalman Filter (EKF) [9]. Such an algorithm computes the observer gains by means of a linearization around the estimated state trajectory of the nonlinear model equations. However, in the case of highly nonlinear systems, as MBSs are, the linearization introduced by the EKF and the related computation of Jacobian matrices can cause significant errors and sometimes may lead to filter instability too.

Therefore, the aim of this paper is to introduce a general theory for the design of nonlinear discrete state observers based on kinematic equations, suitable for MBSs with rigid links and negligible joint clearance. The theory is general in the sense that it can be applied to both open-chain and closed-chain MBSs. The theory also addresses the problem of closed-loop state derivative estimation, which is not trivial when discrete observers are employed, and the problem of computing the estimates in the presence of model singularity, by taking advantage of a switching model.

The theory proposed can make use of both the EKF and the recently introduced observers based on the unscented transformation [9, 10], the so-called Sigma Point Kalman Filters (SPKFs). SPKFs are aimed at overcoming the limitations displayed by the application of the EKF to nonlinear state estimation. In particular, the use of the Spherical Simplex Unscented Kalman Filter (SS-UKF) [9, 11] is evaluated in this paper, as a representative example of SPKF. Indeed, the SS-UKF is very accurate, easy to implement, and similar to the EKF in terms of computational costs. Nonetheless, as previously mentioned, the theory presented can make use of any unscented transformation.

The paper is set out as follows: Sect. 2 briefly outlines the general estimation strategies currently available for nonlinear systems. A general first-order (state-space) formulation suitable for performing kinematic estimation is provided in Sect. 3, where the suggested estimation procedure is presented, too. In Sect. 4, some open issues in kinematic estimation are tackled. In particular, state derivative estimation and state estimation in the presence of model singularity are discussed. Numerical and experimental tests on both closed-chain (1 dof) and open-chain (2 dofs) MBSs are presented in Sect. 5: they prove the soundness of the proposed theory. Finally, concluding remarks are given in Sect. 6.

2 Nonlinear state estimation: state-of-the-art schemes

The synthesis of state observers requires to model systems as a set of first-order, ordinary differential equations (ODEs) relating inputs ($\mathbf{u}$), outputs ($\mathbf{y}$), and state variables ($\mathbf{x}$) as follows:

$$\begin{cases} \dot{\mathbf{x}}(t) = \boldsymbol{f}_c\big(\mathbf{x}(t), \mathbf{u}(t)\big), \\ \mathbf{y}(t) = \boldsymbol{g}\big(\mathbf{x}(t), \mathbf{u}(t)\big) \end{cases} \tag{1}$$

where $\boldsymbol{f}_c$ is a nonlinear differential function, called the system equation, while $\boldsymbol{g}$ is an algebraic function representing the observation model, named the measurement equation. Although physical processes are continuous in time, both sensor measurements and the numerical computation of the estimates are obtained at discrete instants of time because of sampling. Hence, the use of discrete-time filtering is preferred, which is based on modeling both the measurement and system equations as discrete-time processes:

$$\begin{cases} \mathbf{x}_k = \boldsymbol{f}(\mathbf{x}_{k-1}, \mathbf{u}_{k-1}), \\ \mathbf{y}_k = \boldsymbol{g}(\mathbf{x}_k, \mathbf{u}_k). \end{cases} \tag{2}$$

In the equation above, index k denotes the kth time sample, while $\boldsymbol{f}$ is the discrete-time state equation (often referred to as the state transition function), which depends on both its continuous expression $\boldsymbol{f}_c$ and on the discretization scheme adopted.

Several uncertainty sources usually affect both system models (e.g. approximations in the model parameters, unmodeled effects) and measurements (e.g. sensor noise, bad calibration

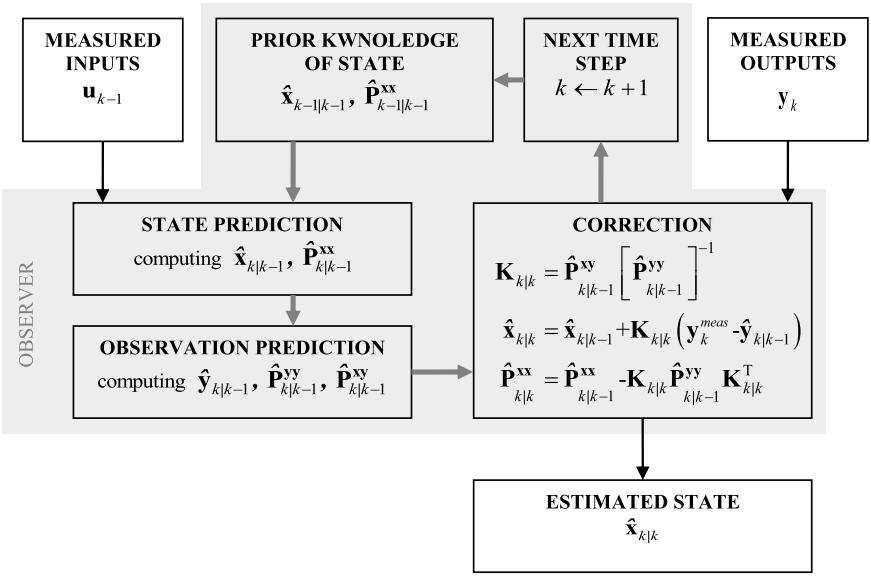

Fig. 1 General scheme of the estimation procedure based on the concept of Kalman filters

or misalignment). Therefore, system equations should include process and measurement noises too, respectively named $\mathbf{v}_k$ and $\mathbf{w}_k$:

$$\begin{cases} \mathbf{x}_k = \boldsymbol{f}(\mathbf{x}_{k-1}, \mathbf{u}_{k-1}, \mathbf{v}_{k-1}), \\ \mathbf{y}_k = \boldsymbol{g}(\mathbf{x}_k, \mathbf{u}_k, \mathbf{w}_k). \end{cases} \tag{3}$$

As a consequence, the state variables should be considered stochastic variables and the estimation problem is often formulated as Bayesian estimation [9]. In order to solve the Bayesian estimation problem, approximate solutions are usually employed. In particular, the most widespread simplification is to assume a Gaussian distribution of noise. This is one of the basic assumptions of Kalman filters, whose general recursive scheme is represented through the block diagram in Fig. 1, which highlights the presence of two macro phases: the prediction and the correction. The block diagram just presents the equations of the correction phase since these equations are general and are required for any estimation scheme. Conversely, the equations for computing the a priori estimates in the prediction phase of the state vector ($\hat{\mathbf{x}}_{k|k-1}$), the input vector ($\hat{\mathbf{y}}_{k|k-1}$) and the covariance matrices ($\hat{\mathbf{P}}^{\mathbf{xx}}_{k|k-1}$, $\hat{\mathbf{P}}^{\mathbf{yy}}_{k|k-1}$, $\hat{\mathbf{P}}^{\mathbf{xy}}_{k|k-1}$), are specific for each filter and are not discussed here. The subscript $k|k-1$ just means that the value refers to the kth time step and it is computed making use of the information available at the time step $k-1$.

The recursive scheme in Fig. 1 shows that an observer corrects the so-called prediction (or a priori estimation), $\hat{\mathbf{x}}_{k|k-1}$, computed through the uncertain model $\boldsymbol{f}$ and the noisy input measurements $\mathbf{u}_{k-1}$ of the previous time step $(k-1)$, by means of the output estimation error $(\mathbf{y}_k - \hat{\mathbf{y}}_{k|k-1})$ weighed through the filter gain $\mathbf{K}_{k|k}$:

$$\hat{\mathbf{x}}_{k|k} = \hat{\mathbf{x}}_{k|k-1} + \mathbf{K}_{k|k}(\mathbf{y}_k - \hat{\mathbf{y}}_{k|k-1}). \tag{4}$$

The estimation error $(\mathbf{y}_k - \hat{\mathbf{y}}_{k|k-1})$ is often referred to as the innovation.

Therefore, the final estimation at the current time step k (a posteriori estimation), $\hat{\mathbf{x}}_{k|k}$, includes both the prediction $\hat{\mathbf{x}}_{k|k-1}$ based on the system model, and the correction $\mathbf{K}_{k|k}(\mathbf{y}_k - \hat{\mathbf{y}}_{k|k-1})$ The latter term behaves as a closed-loop correction, in the control theory sense, forcing the estimation to correctly track sensor measurements by compensating model uncertainty.

In the following subsections, the algorithms used by the EKF and by the SPKFs for computing state and observation predictions are briefly explained to highlight similarities and differences. The interested reader could refer to the quoted references for more detailed discussions.

2.1 Discrete extended Kalman filter

Basically, the EKF is the extension to nonlinear systems of the Kalman filter (KF) [2] originally developed for linear systems. Such an extension is made by directly employing the nonlinear system equations ($\boldsymbol{f}$) and measurement equations ($\boldsymbol{g}$) to perform both the state prediction $\hat{\mathbf{x}}_{k|k-1} = \boldsymbol{f}(\hat{\mathbf{x}}_{k-1|k-1}, \mathbf{u}_{k-1})$ and the observation $\hat{\mathbf{y}}_{k|k-1} = \boldsymbol{g}(\hat{\mathbf{x}}_{k|k-1})$. In contrast, the EFK algorithm replaces the nonlinear model with its Jacobian matrices $\hat{\mathbf{F}}_{k-1|k-1} = \partial \boldsymbol{f}/\partial \mathbf{x}|_{\hat{\mathbf{x}}_{k-1|k-1}, \mathbf{u}_{k-1}}$ (the state transition matrix) and $\hat{\mathbf{H}}_{k|k-1} = \partial \boldsymbol{g}/\partial \mathbf{x}|_{\hat{\mathbf{x}}_{k|k-1}}$ (the observation matrix), computed about the estimated state trajectory, in order to propagate the covariance matrices $\hat{\mathbf{P}}^{\mathbf{xx}}$, $\hat{\mathbf{P}}^{\mathbf{yy}}$, $\hat{\mathbf{P}}^{\mathbf{xy}}$. Such matrices have the following dependence on the covariance matrices of the model and the measurement noises, named respectively $\mathbf{Q}$ and $\mathbf{R}$:

$$\hat{\mathbf{P}}^{\mathbf{xx}}_{k|k-1} = \hat{\mathbf{F}}_{k-1|k-1}\hat{\mathbf{P}}^{\mathbf{xx}}_{k-1|k-1}\hat{\mathbf{F}}^{\mathrm{T}}_{k-1|k-1} + \mathbf{Q}; \qquad \hat{\mathbf{P}}^{\mathbf{yy}}_{k|k-1} = \hat{\mathbf{H}}_{k|k-1}\hat{\mathbf{P}}^{\mathbf{xx}}_{k|k-1}\hat{\mathbf{H}}^{\mathrm{T}}_{k|k-1} + \mathbf{R};$$
$$\hat{\mathbf{P}}^{\mathbf{xy}}_{k|k-1} = \hat{\mathbf{P}}^{\mathbf{xx}}_{k|k-1}\hat{\mathbf{H}}^{\mathrm{T}}_{k|k-1}.$$

Therefore, EKF is based on equations that are optimal only in the case of linear systems, but when nonlinearities are significant, linearization unavoidably leads to large errors, inaccurate estimations, and sometimes to filter instability.

2.2 Sigma point Kalman filters

Another extension of the KF to nonlinear state estimation is the family of the SPKFs. Such observers are based on the idea that "*it should be easier to approximate a Gaussian distribution than it is to approximate an arbitrary nonlinear function*" [10]. The Gaussian distribution of the state variables is approximated by means of a set of weighed sample points (called sigma points) that are selected so as to capture completely the first two moments of a Gaussian distribution. Once the sigma points have been chosen, they are propagated through the actual nonlinear function and are used to approximate the desired statistics with the same accuracy of, at least, the 2nd order Taylor's series expansion [10]. Therefore, SPKFs calculate the statistics of random variables undergoing nonlinear transformations without the need of linearization. Different sigma point selection strategies have been proposed in the literature, such as the Unscented Transformation [10], the Scaled Unscented Transformation [12], the Minimal Skew Simplex Unscented Transformation [13], the Spherical Simplex Unscented Transformation [11]. Each strategy leads to a different number of sigma points and has a different computational cost and numerical accuracy. The selection of the most suitable SPKF depends on the requirements of the specific application (in terms, for example, of computational power available, need for accuracy, presence of noise) and will not be discussed here since it goes beyond the scope of this paper.

The general algorithm used to perform the prediction step with SPKFs is briefly described in the following by means of a matrix formulation, just to explain the basic idea of the SPKFs. Each SPKF formulation is based on a definition of the matrix of the sigma points, $\hat{\mathbf{X}}_{k-1|k-1} = [\hat{\mathbf{x}}_{k-1|k-1}\ \hat{\mathbf{x}}_{k-1|k-1}\ \ldots\ \hat{\mathbf{x}}_{k-1|k-1}] + \sqrt{\hat{\mathbf{P}}^{\mathbf{xx}}_{k-1|k-1}}\boldsymbol{\chi} \in \Re^{N\times p}$, where matrix $\boldsymbol{\chi}$ depends on the sigma point selection strategy. The scalars N and p are respectively the state dimension and the number of sigma points; these two parameters play a crucial role in affecting the computational cost of the estimation. Once the sigma points are defined, both the prediction and the computation of the observer gains are performed through the nonlinear system equations. As for the prediction, the a priori estimates of both the state $\hat{\mathbf{x}}_{k|k-1}$, and the output $\hat{\mathbf{y}}_{k|k-1}$ are computed as the weighed sum of the sigma points propagated through the nonlinear functions $\boldsymbol{f}$ and $\boldsymbol{g}$:

$$\begin{aligned} &\hat{\mathbf{x}}_{k|k-1} = \hat{\mathbf{X}}_{k|k-1}\mathbf{w}, \qquad \hat{\mathbf{y}}_{k|k-1} = \hat{\mathbf{Y}}_{k|k-1}\mathbf{w}, \\ &\hat{\mathbf{X}}_{k|k-1} = \boldsymbol{f}(\hat{\mathbf{X}}_{k-1|k-1}, \mathbf{u}_{k-1}) \in \Re^{N\times p}, \qquad \hat{\mathbf{Y}}_{k|k-1} = \boldsymbol{g}(\hat{\mathbf{X}}_{k|k-1}) \in \Re^{o\times p}. \end{aligned} \tag{5}$$

In the previous set of equations, $\mathbf{w} \in \Re^p$, $\mathbf{w} = \{w_0\ w_1\ \ldots\ w_p\}^{\mathrm{T}}$, is the vector of the sigma point weights (which depend on the sigma point selection strategies) while o represents the number of output variables. For shortness of notation the functions $\boldsymbol{f}$ and $\boldsymbol{g}$ have been redefined in Eq. (5) as $\boldsymbol{f} : \Re^{N\times p} \mapsto \Re^{N\times p}$ and $\boldsymbol{g} : \Re^{o\times p} \mapsto \Re^{o\times p}$, meaning that matrix $\hat{\mathbf{X}}_{k|k-1}$ is obtained applying function f to each column of $\hat{\mathbf{X}}_{k-1|k-1}$, for example, the ith column of $\hat{\mathbf{X}}_{k|k-1}$ is obtained as $\hat{\mathbf{X}}^i_{k|k-1} = f(\hat{\mathbf{X}}^i_{k-1|k-1}, \mathbf{u}_{k-1})$.

The covariance matrices for the synthesis of the filter gain $\mathbf{K}_{k|k}$ are computed on the basis of the previously defined values $\hat{\mathbf{X}}_{k|k-1}$ and $\hat{\mathbf{Y}}_{k|k-1}$ as follows:

$$\begin{aligned} &\hat{\mathbf{P}}^{\mathbf{xx}}_{k|k-1} = \hat{\mathbf{X}}_{k|k-1}\mathbf{W}_{\mathrm{c}}\hat{\mathbf{X}}^{\mathrm{T}}_{k|k-1} + \mathbf{Q}; \qquad \hat{\mathbf{P}}^{\mathbf{yy}}_{k|k-1} = \hat{\mathbf{Y}}_{k|k-1}\mathbf{W}_{\mathrm{c}}\hat{\mathbf{Y}}^{\mathrm{T}}_{k|k-1} + \mathbf{R}; \\ &\hat{\mathbf{P}}^{\mathbf{xy}}_{k|k-1} = \hat{\mathbf{X}}_{k|k-1}\mathbf{W}_{\mathrm{c}}\hat{\mathbf{Y}}^{\mathrm{T}}_{k|k-1} \end{aligned}$$

with the weights represented as $\mathbf{W}_{\mathrm{c}} = [\mathbf{I} - \mathbf{W}_{\mathrm{m}}]\,\mathrm{diag}(\mathbf{w})[\mathbf{I} - \mathbf{W}_{\mathrm{m}}]$,

$$\mathbf{W}_{\mathrm{m}} = \begin{bmatrix} \mathbf{w} & \mathbf{w} & \ldots & \mathbf{w} \end{bmatrix} \in \Re^{p\times p}.$$

Among the several sigma point selection strategies proposed for the unscented transformation, in this paper the one called spherical simplex sigma point selection is adopted as a representative sample [11], which leads to the so-called Spherical Simplex Unscented Kalman Filters (SS-UKF). Such a strategy provides an effective trade-off between computational cost and overall effectiveness [4]. Indeed, this unscented transformation selects $p = N + 2$ sigma points lying on a hypersphere whose radius is proportional to $\sqrt{N}$, where N is the state dimension.

2.3 Non-stochastic interpretation of Kalman filters

Both the SPKFs and the EKFs, previously discussed, perform the so-called stochastic state estimation, and therefore require the knowledge of the zero-mean Gaussian noise covariance matrices $\mathbf{Q}$ and $\mathbf{R}$ to compute the filter gains. Since, in practice, noise is often non-Gaussian (in particular the model noise, whose covariance is also difficult to be evaluated), these filters can be also seen in a non-stochastic way by considering matrices $\mathbf{Q}$ and $\mathbf{R}$ as design parameters to be tuned for optimizing performances, rather than actual properties of the disturbance.

3 Kinematic modeling of multibody systems: state-space formulation of kinematic models

3.1 The kinematic model

The basic idea behind kinematic estimation is to exploit kinematic models, based on kinematic constraint equations, and a proper set of measurable kinematic variables in order to estimate other unmeasured kinematic variables. Let us consider an arbitrary open-chain or closed-chain MBS with rigid links, joints with no clearance and holonomic, scleronomous constraints. In order to perform estimation through the proposed approach, the system should be modeled through a suitable set of n independent coordinates $\mathbf{z}$ (n is the number of degrees of freedom, dofs), and a set of m dependent coordinates $\mathbf{h}$ to be measured at some order of derivative (as it will be discussed later in Sect. 3.2). A set of m algebraic constraint equations relating the dependent and the independent coordinates can be hence defined:

$$\mathbf{\Phi}(\mathbf{z}, \mathbf{h}) = \mathbf{0}. \tag{6}$$

Such an equation is a set of nonlinear equations in the variables $\mathbf{z}$ and $\mathbf{h}$, and does not depend explicitly on time in the case of scleronomous constraints. By differentiating Eq. (6) with respect to time, the following velocity and acceleration equations are obtained:

$$\dot{\mathbf{h}} = \mathbf{S}(\mathbf{z})\dot{\mathbf{z}}, \tag{7}$$

$$\ddot{\mathbf{h}} = \mathbf{S}(\mathbf{z})\ddot{\mathbf{z}} + \dot{\mathbf{S}}(\mathbf{z}, \dot{\mathbf{z}})\dot{\mathbf{z}}. \tag{8}$$

Matrices $\mathbf{S}$ and $\dot{\mathbf{S}} \in \mathbb{R}^{m \times n}$ are the sensitivity coefficient matrix and its time derivative, respectively. In practice, the columns of matrix $\mathbf{S}$ constitute a basis of the nullspace of the Jacobian matrix of the constraint equation [14], and just depend on the mechanism position.

Equations (6), (7) and (8) define the kinematic model.

3.2 First-order model formulation

In order to be useful to state estimation, the kinematic model defined in the previous section must be reformulated as first-order ODEs to fit the model of Eq. (1). To this end, proper definitions of the state vector $\mathbf{x}$, the system measured input vector $\mathbf{u}$, and the measured output vector $\mathbf{y}$ are crucial. Such definitions must ensure both model existence and the observability of the system model realization.

As far as the state vector is concerned, it is defined as a $2n$-dimensional vector including both the independent coordinates and their first derivatives:

$$\mathbf{x} = \{\mathbf{z} \quad \dot{\mathbf{z}}\}^{\mathrm{T}}. \tag{9}$$

As for the model input vector $\mathbf{u}$, it should include at least n independent measured accelerations.

After these preliminary definitions of the state and the inputs, it is possible to define the first-order ODEs representing a MBS in the kinematic estimation. Such a model is inferred from the acceleration equation (8):

$$\dot{\mathbf{x}} = \begin{Bmatrix} \dot{\mathbf{z}} \\ \ddot{\mathbf{z}} \end{Bmatrix} = \begin{Bmatrix} \dot{\mathbf{z}} \\ [\mathbf{S}^{\mathrm{T}}(\mathbf{z})\mathbf{S}(\mathbf{z})]^{-1}\mathbf{S}^{\mathrm{T}}(\mathbf{z})\{\mathbf{u} - \dot{\mathbf{S}}(\mathbf{z}, \dot{\mathbf{z}})\dot{\mathbf{z}}\} \end{Bmatrix}. \tag{10}$$

In Eq. (10), the model input $\mathbf{u}$ is the m-dimensional vector of the sensed accelerations, $\mathbf{u} = \ddot{\mathbf{h}}$ ($m \geq n$, n being the number of dofs). It is worth noticing that, in kinematic estimation, the

accelerations $\ddot{\mathbf{h}}$ play the same role as the forces (or torques) in the traditional synthesis of state observers based on dynamic models, where the input vector collects the external actuation and disturbance forces.

The model obtained in Eq. (10) clearly shows that the choice of the system inputs affects the existence of the system model, since it sets the existence of matrix $[\mathbf{S}^{\mathrm{T}}(\mathbf{z})\mathbf{S}(\mathbf{z})]^{-1}$.

3.3 Definition of the output vector

In order to set the measurement equation $\boldsymbol{g}$, the output vector $\mathbf{y}$ should be defined by selecting a set of other additional measured variables adequate ensuring system observability even in the presence of relevant uncertainty on the model and on the state initial estimates. The concept of observability can be simplified as the issue of whether the state of a system, whose model is known, is uniquely determinable from its measured inputs and outputs, and the initial conditions [15]. The estimation error is therefore asymptotically stable if the system satisfies the observability condition and if the initial estimation error, as well as the disturbance noise terms, are small enough [16, 17].

The number of the independent measured variables in $\mathbf{y}$ should be at least equal to the number of system dofs, n. Although a rigorous discussion of observability is beyond the aims of the paper, some general rules for selecting the output vector are here provided. Generally speaking, a set of sensors ensuring adequate observability even in the presence of uncertain state initial conditions and of model noise (i.e. modeling errors) should include as many non-redundant position measurements as the number of dofs, since such measurements are able to capture the zero-frequency dynamics and hence prevent estimation drifts.

Once the variables in $\mathbf{y}$ have been selected, the measurement equation $\mathbf{g}$ is established. Function $\boldsymbol{g}$ is a set of algebraic equations relating the output variables $\mathbf{y}$ and the state $\mathbf{x}$, and hence its formulation is obtained through Eqs. (6) and (7).

Finally, it is worth highlighting the different role played in the estimation process by the measured variables collected in $\mathbf{u}$ and those in $\mathbf{y}$. Indeed, the variables in $\mathbf{y}$ intervene in the correction phase by contributing to the filter innovation, which is the discrepancy between the measurements predicted through the nominal model and the actual ones (see Sect. 2). In contrast, the variables in $\mathbf{u}$ play a key role in allowing the correct model formulation and the existence of $[\mathbf{S}^{\mathrm{T}}(\mathbf{z})\mathbf{S}(\mathbf{z})]^{-1}$, without contributing to the filter innovation. They intervene in just the prediction phase.

From the considerations made so far it is apparent that at least $2n$ non-redundant measurements are collected in vectors $\mathbf{u}$ and $\mathbf{y}$, to properly perform state estimations in the prediction–correction way typical of the closed-loop observers here discussed. In Sect. 4.1, it will be shown that, by following the original approach here proposed, the same set of measurements allows performing also state derivative estimation.

3.4 Discrete-time representation of the filter ODEs

As previously discussed in Sect. 2, the use of discrete-time filtering is very common in practice. Therefore, the first-order ODEs of the kinematic model stated in Eq. (10) should be represented as a discrete-time process. A typical discrete-time general representation of the state-space model is shown in Eq. (2). As far as the discretization scheme is concerned, most of the works in the literature on state observers usually perform model discretization through the first-order Euler's method, since its implementation is straightforward and it usually requires small computational efforts. In the case of MBSs, in order to handle the significant nonlinearities due to kinematic constraints, a great improvement can be obtained by adopting the single-step higher order numerical techniques developed for the numerical

integration of the equations of motion [14]. Indeed, higher order methods usually allow improving accuracy and getting a larger region of absolute stability, even in the presence of a larger sample time.

The following is an adequately general expression which can be employed to represent a discrete-time model, in the case of a wide number of both implicit (e.g. the trapezoidal rule) and explicit (e.g. Runge–Kutta) techniques, leading to similar expressions of the discrete state transition function $\boldsymbol{f}$ [14]:

$$\mathbf{x}_k = \mathbf{x}_{k-1} + \Delta t \sum_{i=1}^{\nu} \beta_i \kappa_i, \quad \kappa_i = \boldsymbol{f}_c \left(\mathbf{x}_{k-1} + \Delta t \sum_{j=1}^{\nu} \lambda_{ij} \kappa_j, \mathbf{u}_{k-1} \right). \tag{11}$$

The parameters β_i, λ_{ij} and ν are peculiar to the specific discretization scheme adopted. Yet, the approach to state estimation proposed in this paper does not impose any specific discretization scheme, and therefore any other method leading to a model representation slightly different from the one in Eq. (11) can be adopted.

As for the discretization of the measurement equation $\boldsymbol{g}$, it does not represent a critical issue since $\boldsymbol{g}$ is an algebraic equation.

Once the model formulated in Eq. (10) is discretized and the output vector is defined, the observer synthesis can be performed through the methods discussed in Sect. 2. The whole procedure discussed represents a general and consistent approach to state estimation of kinematic variables.

4 Nonlinear state estimation for MBSs: critical issues

4.1 State derivative estimation with discrete-time observers

The use of discrete-time filters based on the model in Eq. (2) allows estimating the state of a MBS once the system model, the inputs, the outputs, and the initial state vector are known. Conversely, state derivative estimation (i.e. acceleration estimation) with the prediction–correction scheme proposed in Fig. 1 is less straightforward with discrete schemes. Indeed, it imposes to include all the variables to be estimated within the state, and consequently, to augment the set of the continuous-time first-order ODEs in Eq. (10) with some relations involving variables of a greater derivative order. Therefore, accelerations should be included in the augmented state vector, denoted $\mathbf{x}^{aug}$, and consequently, the set of first-order ODEs must be augmented with some relations involving also jerks. This implies that, at least theoretically, jerk should be measured and included within the system input vector. Indeed, the input vector of a kinematic model includes kinematic quantities having the same time-derivative order of the components of $\dot{\mathbf{x}}$ with the highest derivative order. This is clearly unfeasible in the case of acceleration estimation.

As two alternative approaches to acceleration estimation, discrete-time state estimations can be computed through open-loop estimation with no prediction–correction iterations, either by means of numerical derivatives of the state variables or by means of the solution of the acceleration equations. Since no correction is performed, these approaches may be inaccurate because they are respectively affected by sensor noise and model uncertainty.

In order to perform accurate discrete-time closed-loop state derivative estimations with the prediction–correction iterations, the equations representing the state derivative should be included in the state transition function $\boldsymbol{f}$, so that the correction $\mathbf{K}_{k|k}(\mathbf{y}_k^{meas} - \hat{\mathbf{y}}_{k|k-1})$ is applied to compensate for measurement noise or model uncertainty. To this purpose, this

section proposes three alternative approaches which embed the state derivative equations into the state transition function. In particular, the first approach includes the acceleration equations in $\boldsymbol{f}$ and is therefore suitable in the case of noisy measurements that do not allow effective numerical derivative without introducing delay due to low-pass causal filters. On the other hand, the second approach is chiefly based on numerical derivatives whose scheme is, however, included into $\boldsymbol{f}$: it is hence suggested in the presence of considerable model uncertainty. Finally, the third approach combines the advantages of the previous ones, at the cost of a slight increase in the model formulation complexity.

4.1.1 Acceleration equations with random walk

The acceleration equations in Eq. (8) cannot be expressed as discrete-time state-space equations if acceleration belongs to the state, and therefore are not suitable to be employed in the observer model straightforwardly. To overcome this limitation, acceleration is modeled through a so called "random walk":

$$\ddot{\mathbf{z}}_k = \ddot{\mathbf{z}}_{k-1} + \delta_{k-1} \tag{12}$$

where δ_{k-1} is the noise vector, representing the uncertainty on this equation, usually assumed as white noise. Basically, this approach assumes that the current value of the acceleration vector $\ddot{\mathbf{z}}_k$ is equal to the previous one $\ddot{\mathbf{z}}_{k-1}$ plus a noise terms δ_{k-1}. The use of random walk is a trick often adopted for approximating the model of unknown, or highly uncertain, dynamics. Then, by making explicit the acceleration equations in Eq. (8), Eq. (12) can be rewritten in the following form:

$$\ddot{\mathbf{z}}_k = \left[\mathbf{S}_{k-1}^{\mathrm{T}}\mathbf{S}_{k-1}\right]^{-1}\mathbf{S}_{k-1}^{\mathrm{T}}\{\ddot{\mathbf{h}}_{k-1} - \dot{\mathbf{S}}_{k-1}\dot{\mathbf{z}}_{k-1}\} + \delta_{k-1}. \tag{13}$$

This approach casts the acceleration equations as first-order difference equations, by taking also advantage of the probabilistic nature of the state observer.

The system model adopted in the estimation of the augmented state $\mathbf{x}^{aug} = \{\mathbf{x}^{\mathrm{T}}\ \ddot{\mathbf{z}}^{\mathrm{T}}\}^{\mathrm{T}}$ is therefore represented through the following system of equations, originated from Eqs. (10) and (13):

$$\mathbf{x}_k^{aug} = \begin{Bmatrix} \mathbf{x}_k \\ \ddot{\mathbf{z}}_k \end{Bmatrix} = \begin{Bmatrix} \boldsymbol{f}(\mathbf{x}_{k-1}, \ddot{\mathbf{h}}_{k-1}) \\ [\mathbf{S}_{k-1}^{\mathrm{T}}\mathbf{S}_{k-1}]^{-1}\mathbf{S}_{k-1}^{\mathrm{T}}\{\ddot{\mathbf{h}}_{k-1} - \dot{\mathbf{S}}_{k-1}\dot{\mathbf{z}}_{k-1}\} \end{Bmatrix} = \boldsymbol{f}_{aug}\left(\mathbf{x}_{k-1}^{aug}, \ddot{\mathbf{h}}_{k-1}\right). \tag{14}$$

4.1.2 Numerical derivative with model uncertainty

An alternative approach to acceleration estimation embeds in the system model a set of first-order difference equations ψ representing the numerical derivation, in the presence of noise δ_k:

$$\ddot{\mathbf{z}}_k = \psi(\dot{\mathbf{z}}_k, \mathbf{z}_k, \ddot{\mathbf{z}}_{k-1}, \dot{\mathbf{z}}_{k-1}, \mathbf{z}_{k-1}) + \delta_{k-1}. \tag{15}$$

The estimation of the augmented state $\mathbf{x}^{aug} = \{\mathbf{x}^{\mathrm{T}}\ \ddot{\mathbf{z}}^{\mathrm{T}}\}^{\mathrm{T}}$ is therefore performed through the following model:

$$\begin{Bmatrix} \mathbf{I}\mathbf{x}_k \\ \Psi_l(\mathbf{x}_k, \ddot{\mathbf{z}}_k) \end{Bmatrix} = \begin{Bmatrix} \boldsymbol{f}(\mathbf{x}_{k-1}, \mathbf{u}_{k-1}) \\ \Psi_r(\mathbf{x}_{k-1}, \ddot{\mathbf{z}}_{k-1}) \end{Bmatrix} = \boldsymbol{f}_{aug}\left(\mathbf{x}_{k-1}^{aug}, \mathbf{u}_{k-1}\right) \tag{16}$$

where $\mathbf{I}$ is the identity matrix, while functions Ψ_l and Ψ_r are obtained from Ψ by splitting the current state and the one at the previous time step $(k-1)$. Having introduced the numerical derivation scheme in the observer, the error due to measurement noise and to the

approximate nature of numerical derivation is partially compensated by the closed-loop correction. Such a correction behaves as an optimal nonlinear filter whose gains, and therefore bandwidth, are updated at each time step depending on the estimation error and on noise, in accordance with the theory discussed in Sect. 2.

For instance, following a very popular approach in multibody system dynamics, the Newmark's first-order interpolation method [14] can be employed as a derivative scheme for accelerations:

$$\ddot{\mathbf{z}}_k = \frac{1}{\beta \Delta t^2}(\mathbf{z}_k - \mathbf{z}_{k-1}) - \frac{1}{\beta \Delta t}\dot{\mathbf{z}}_{k-1} + \left(1 - \frac{1}{2\beta}\right)\ddot{\mathbf{z}}_{k-1}, \tag{17}$$

or alternatively,

$$\ddot{\mathbf{z}}_k = \frac{\dot{\mathbf{z}}_k - \dot{\mathbf{z}}_{k-1}}{\gamma \Delta t} + \frac{\gamma - 1}{\gamma}\ddot{\mathbf{z}}_{k-1}. \tag{18}$$

In Eqs. (17) and (18), Δt is the sample time adopted in the estimation (which can be different from the ones of sensor measurements in the case of multi-rate estimation). β and γ are positive parameters defining the derivation method.

Compared with the model-based method in Sect. 4.1.1, this approach is more effective in the presence of considerable model uncertainty, while it introduces high-frequency errors in the presence of noisy sensors. Nevertheless, the low-pass filtering due to the correction ensures that such high-frequency errors are smaller than the ones obtained through open-loop numerical derivatives.

4.1.3 Acceleration equations with numerical derivative

A third approach is proposed in this paper and is basically obtained by merging the two techniques presented above, in order to improve the overall estimation by reducing model uncertainty through kinematic modeling, a numerical derivative scheme, and the correction provided by the filter. The method consists in writing explicitly the state derivative at step $k-1$ (i.e. $\ddot{\mathbf{z}}_{k-1}$ in the acceleration estimation) through the acceleration equations relating state, state derivative and inputs at time step $k-1$:

$$\ddot{\mathbf{z}}_{k-1} = \left[\mathbf{S}_{k-1}^{\mathrm{T}}\mathbf{S}_{k-1}\right]^{-1}\mathbf{S}_{k-1}^{\mathrm{T}}\{\ddot{\mathbf{h}}_{k-1} - \dot{\mathbf{S}}_{k-1}\dot{\mathbf{z}}_{k-1}\}. \tag{19}$$

By taking advantage of the numerical derivative scheme in Eq. (18), the following set of equations augments the system model:

$$\ddot{\mathbf{z}}_k = \frac{\dot{\mathbf{z}}_k - \dot{\mathbf{z}}_{k-1}}{\gamma \Delta t} + \frac{\gamma - 1}{\gamma}\left[\mathbf{S}_{k-1}^{\mathrm{T}}\mathbf{S}_{k-1}\right]^{-1}\mathbf{S}_{k-1}^{\mathrm{T}}\{\mathbf{u}_{k-1} - \dot{\mathbf{S}}_{k-1}\dot{\mathbf{z}}_{k-1}\} + \delta_{k-1}. \tag{20}$$

For instance, if the EKF is employed for the estimation, and the Newmark's method is adopted, the accelerations are estimated as follows (the hat denotes the estimated values):

$$\hat{\ddot{\mathbf{z}}}_k = \frac{\hat{\dot{\mathbf{z}}}_k - \hat{\dot{\mathbf{z}}}_{k-1}}{\gamma \Delta t} + \frac{\gamma - 1}{\gamma}\left[\mathbf{S}_{k-1}^{\mathrm{T}}\mathbf{S}_{k-1}\right]^{-1}\mathbf{S}_{k-1}^{\mathrm{T}}\{\mathbf{u}_{k-1} - \dot{\mathbf{S}}_{k-1}\hat{\dot{\mathbf{z}}}_{k-1}\} + \mathbf{K}_{k|k}(\mathbf{y}_k - \hat{\mathbf{y}}_{k|k-1}). \tag{21}$$

4.2 Estimation in the presence of model singularity

In Sect. 3, the importance of a proper definition of the system inputs has been discussed, since the existence of matrix $[\mathbf{S}^{\mathrm{T}}(\mathbf{z})\mathbf{S}(\mathbf{z})]^{-1}$ depends on the choice of such variables. Indeed,

the set of input variables may lead to some configurations where matrix $[\mathbf{S}^{\mathrm{T}}(\mathbf{z})\mathbf{S}(\mathbf{z})]$ is singular, and therefore the system model in Eq. (10), (explicitly representing $\dot{\mathbf{x}}$ as a function of $\mathbf{u}$) cannot be formulated. These configurations will be hereafter denoted as "model singularities". In practice, the system input cannot be employed to reconstruct the state variables in these configurations.

Although a good selection of the sensor position and the use of sensor redundancy allow solving this occurrence, a solution based on the use of a switching model is proposed in this work to overcome this issue whenever the definition of the input vector is restricted by technical or economical constraints. Switching models are widely and effectively employed in control theory to approximate more complicate models in the synthesis of controllers or estimators (see, e.g. [1]). In particular, whenever the system is in the neighborhood of a singular configuration, the kinematic model defined in Sects. 2 and 3 is switched to a random walk model with Gaussian noise, which provides an approximation of the actual one.

Let Ω_s be the set of the singular configurations,

$$\Omega_s(\mathbf{z}) = \left\{\mathbf{z} \mid \det\left(\mathbf{S}^{\mathrm{T}}\mathbf{S}\right) = 0\right\}, \tag{22}$$

and let Ω be a set including Ω_s ($\Omega_s \subset \Omega$), which represents the so-called switching rule, then the following first-order discrete switching model is defined:

$$\mathbf{x}_k = \begin{cases} \boldsymbol{f}(\mathbf{x}_{k-1}, \mathbf{u}_{k-1}, \mathbf{v}_{k-1}) & \text{if } \mathbf{z}_{k-1} \notin \Omega, \\ \mathbf{x}_{k-1} + \delta_{k-1} & \text{if } \mathbf{z}_{k-1} \in \Omega. \end{cases} \tag{23}$$

By taking advantage of the representation in Eq. (11), Eq. (23) can be also written as follows, to provide a clearer sample representation of the switching model:

$$\mathbf{x}_k = \begin{cases} \mathbf{x}_{k-1} + \Delta t \sum_{i=1}^{r} \beta_i \kappa_i + \boldsymbol{v}_{k-1} & \text{if } \mathbf{z}_{k-1} \notin \Omega, \\ \mathbf{x}_{k-1} + \delta_{k-1} & \text{if } \mathbf{z}_{k-1} \in \Omega. \end{cases} \tag{24}$$

The simplest choice for Ω is to define it as just a function of the position,

$$\Omega(\mathbf{z}) = \left\{\mathbf{z} \;\middle|\; \left|\det\left(\mathbf{S}^{\mathrm{T}}\mathbf{S}\right)\right| \leq \varepsilon\right\}, \tag{25}$$

where ε is a suitably small threshold, usually approaching zero. More effectively, in order to prevent chattering and instability by operating in the slow switching condition, hysteresis can be employed in the switching rule by means of a redefinition of Ω as a function of both position and speed ($\Omega(\mathbf{z}, \dot{\mathbf{z}})$).

5 Numerical and experimental results

Two tests are proposed to prove the effectiveness of the theory developed. The first test is numerical and involves a single-dof, closed-chain, planar mechanism (slider–crank mechanism). The second one is experimental: the estimation approach proposed is applied to an open chain, two-dof, two-link, planar mechanism.

5.1 Test case I: slider–crank mechanism

The kinematic scheme of the slider–crank mechanism adopted in the first test case is shown in Fig. 2. The aim of the test is estimating the angular velocity and acceleration of the

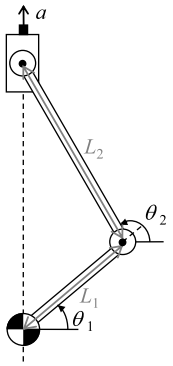

Fig. 2 Kinematic scheme of a slider–crank mechanism

crank, as it is often useful in practice, since feedback motion controllers often require precise knowledge of speed and acceleration in order to ensure high bandwidth control. Indeed, when no estimator is implemented, angular velocities and accelerations are computed by numerical derivatives and low pass filtering. However, this approach introduces a phase-lag that reduces the controlled system phase margin, and therefore downgrades the bandwidth considerably. Synthesizing an estimator following the proposed approach can greatly improve controller performances.

In order to estimate the angular acceleration of the crank, the augmented state vector $\mathbf{x}^{aug}$ is defined, in accordance with the discussion provided in Sect. 4.1, as $\mathbf{x}^{aug} = \{\theta_1\ \dot{\theta}_1\ \ddot{\theta}_1\}^{\mathrm{T}}$, where θ_1 is the crank rotation. The system is supposed to be equipped with an incremental encoder and a mono-axial accelerometer, measuring respectively the crank angular position θ_1 and the slider linear acceleration a. The measured acceleration (a) is the system input for the estimation: $u = a$. The encoder measurement is instead the measured output, $y = \theta_1$. As far as the system model is concerned, a switching model is adopted in order to yield estimates even close to the model singular configuration, which is encountered whenever the crank is aligned to the connecting link, i.e. $\Omega_s = \{\theta_1 \mid \theta_1 = \theta_2 + k\pi\}$, $k \in \mathbb{N}$. The resulting state-space model takes the following form, if discretized through the first-order Euler's method:

$$
\begin{aligned}
&\begin{Bmatrix} \theta_{1_k} \\ \dot{\theta}_{1_k} \\ \ddot{\theta}_{1_k} \end{Bmatrix} = \nearrow \\
&\qquad \text{if } \theta_{1_{k-1}} \in \Omega \supset \Omega_s \\
&\qquad \begin{Bmatrix}
\theta_{1_{k-1}} + \Delta t \dot{\theta}_{1_{k-1}} \\
\dot{\theta}_{1_{k-1}} + \Delta t \Big(\frac{\sin(a\cos(-\frac{L_1}{L_2}\cos(\theta_{1_{k-1}})))}{L_1 \sin(a\cos(-\frac{L_1}{L_2}\cos(\theta_{1_{k-1}})) - \theta_{1_{k-1}})} a_{k-1} + \cdots \\
\qquad \cdots \frac{L_2 K^2_{\theta_2 \theta_{1,k-1}} + L_1 \cos(a\cos(-\frac{L_1}{L_2}\cos(\theta_{1_{k-1}})) - \theta_{1_{k-1}})}{L_1 \sin(a\cos(-\frac{L_1}{L_2}\cos(\theta_{1_{k-1}})) - \theta_{1_{k-1}})} \dot{\theta}^2_{1_{k-1}} \Big) \\
(\dot{\theta}_{1_k} - \dot{\theta}_{1_{k-1}})/\Delta t + \delta_{k-1}
\end{Bmatrix} \\
&\qquad \text{if } \theta_{1_{k-1}} \notin \Omega \supset \Omega_s \\
&\qquad \begin{Bmatrix}
\theta_{1_{k-1}} + \Delta t \dot{\theta}_{1_{k-1}} \\
\dot{\theta}_{1_{k-1}} + \Delta t \ddot{\theta}_{1_{k-1}} \\
\ddot{\theta}_{1_{k-1}} + \delta_{k-1}
\end{Bmatrix} \\
&\mathrm{y}_k = \begin{bmatrix} 1 & 0 & 0 \end{bmatrix} \mathbf{x}^{aug}_k
\end{aligned}
\tag{26}
$$

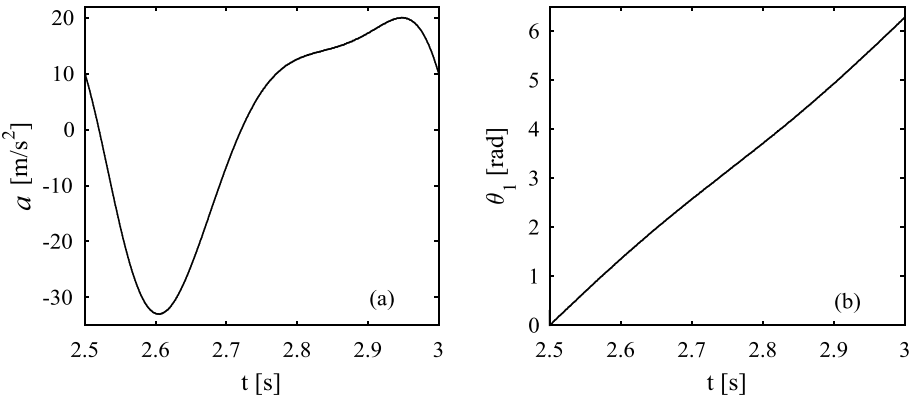

Fig. 3 Simulated noisy measurements: slider acceleration (**a**) and crank angular position (**b**)

where $K_{\theta_2\theta_{1,k-1}} = \frac{\partial\theta_2}{\partial\theta_1}|_{k-1}$ is the sensitivity coefficient, and Δt is the discretization time step (which has been set equal to 1 ms in the numerical simulation).

The switching rule is defined as $\Omega = \{\theta_1 \mid |\theta_1 - (\theta_2 + k\pi)| \leq 0.08 \text{ rad}\}$.

Simulations have been carried out to assess the capability of different estimation strategies to deliver accurate estimations in the presence of measurement and model uncertainties.

A simulation lasting 30 seconds has been tested, which highlights that no drift affects the estimation, i.e. the system is stable (in the control theory sense). The crank speed is obtained as the superposition of a constant-speed signal (12.56 rad/s) and a 2 Hz harmonic signal (whose amplitude is 1.256 rad/s). Two sample portions of the time history of the simulated accelerometer and encoder signals are shown respectively in Figs. 3(a) and 3(b). Measurement noise has been added on both the encoder and the accelerometer signals to try reproducing more realistic conditions. In particular, Gaussian noises have been generated with amplitudes of, respectively, 0.003 rad for the encoder (corresponding to the resolution of a 2000 ppr encoder) and 0.03 m/s^2 for the accelerometer (corresponding to the resolution provided by an accelerometer with sensitivity 10 mV/m s^{-2}, whose signal is converted by a 16-bit ADC with input range of ± 10 V). These values are typical of industrial off-the-shelf devices, and hence represent a meaningful test case. If higher noise affects the measurements, the filter should be properly tuned to obtain the optimal trade-off between noise rejection, accuracy and fast response (i.e. with negligible time delay).

The estimated angular velocity and acceleration of the crank are respectively shown in Figs. 4(a) and 4(b). Estimation has been carried out using both the EKF and the SS-UKF observers, which are assumed as two representative examples of filters. The theory is, however, general enough to allow the use of other filters. As far as acceleration estimation is concerned, the scheme proposed in Sect. 4.1.2, i.e. the one based on numerical derivative, has been adopted. The estimates obtained are also compared with the actual velocity and acceleration computed analytically, i.e. those with no measuring noise. In particular, the errors between the estimated values and the actual ones are plotted in Figs. 4(c) and 4(d) to provide clearer evidence of the estimation accuracy. The error diagrams show that both observers lead to good velocity and acceleration estimations when the mechanism is far from model singularities, which are crossed at time instants 2.62 s and 2.88 s. When singularities are crossed, estimates become less accurate, but still acceptable.

In particular, the use of the SS-UKF is marginally affected by singularity, especially in the estimation of speed. The SS-UKF superiority can be traced back, first of all, to the

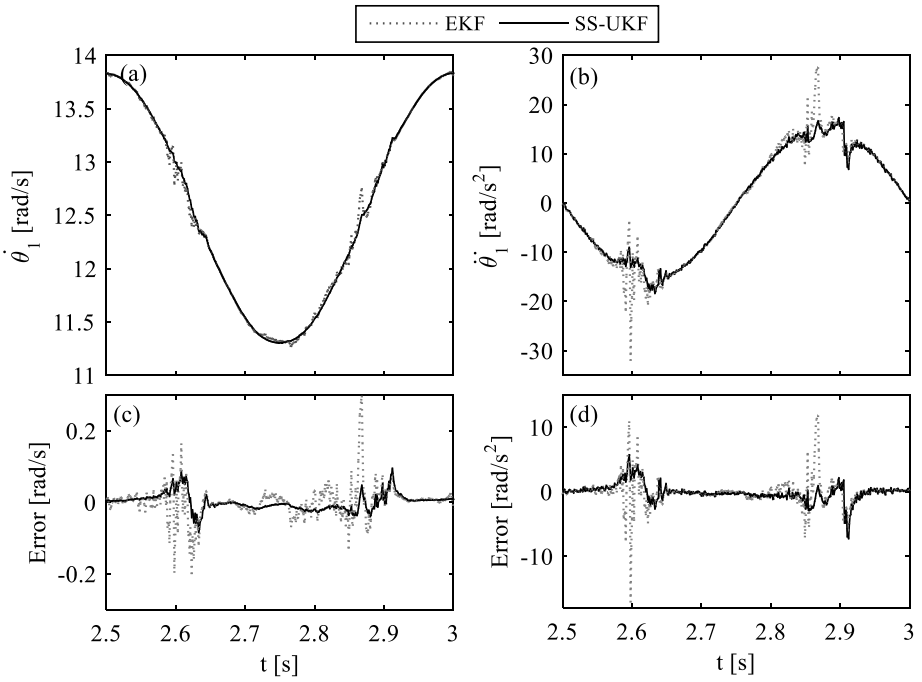

Fig. 4 Estimated crank angular velocity (**a**) and acceleration (**b**). Velocity (**c**) and acceleration (**d**) estimation errors

fact that it does not use any linearization and therefore does not require any Jacobian, whose computation is critical at the model switch, since in such instants the model is not ensured to be derivable. Additionally, the SS-UKF compute the prediction as the weighed sum of more solutions related to different mechanism configurations (in term of positions, velocities, and, in this example, accelerations), rather than just solving the uncertain system model in a single configuration. All these considerations justify the superiority of this class of nonlinear observers to handle such nonlinear problems.

5.2 Test case II: experimental two dof planar mechanism

The laboratory setup shown in Fig. 5(a) has been employed for the experimental validation of the theory developed. The system is an open-chain, planar mechanism with two links, two revolute joints, and therefore two dofs. This MBS recalls a typical planar underactuated manipulator: the shoulder joint is the sole actuated joint, driven by a DC servomotor, while the elbow joint B is passive.

Two incremental encoders (with resolution 1000 ppr) measure the link rotations of both the joints, while two MEMS mono-axial accelerometers (whose sensitivities are 101.9 mV $(\mathrm{m/s^2})^{-1}$ for the accelerometer on link 1 and 6.81 mV $(\mathrm{m/s^2})^{-1}$ for the one on link 2) are mounted to each link for measuring the acceleration in the direction orthogonal to the link itself.

In a manipulator like this one, state estimation could be useful, for instance, in the synthesis of advanced state feedback controllers (see, e.g. [18]), which require accurate knowledge

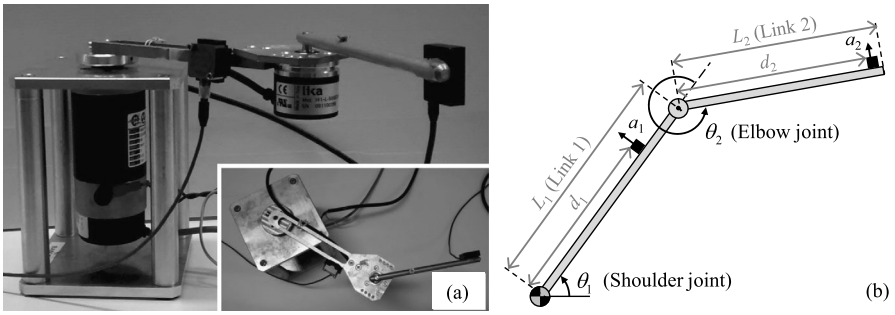

Fig. 5 (**a**) Pictures of the instrumented two-dof planar manipulator (seen from one side and above); (**b**) Kinematic scheme of the manipulator

of the joint speed and sometimes also acceleration. Yet, the direct measurement of such variables is unfeasible, and should be replaced by a suitable estimation.

To estimate the acceleration, the state vector has been augmented (see Sect. 4.1) and defined as $\mathbf{x}^{aug} = \{\theta_1\ \theta_2\ \dot{\theta}_1\ \dot{\theta}_2\ \ddot{\theta}_1\ \ddot{\theta}_2\}^{\mathrm{T}}$, with the obvious meaning for the symbols (see Fig. 5(b)). The discrete state-space formulation of the kinematic model, obtained by discretizing the continuous-time equations through the first-order Euler's method, is the following one:

$$\mathbf{x}_k^{aug} = \begin{Bmatrix} \theta_1 \\ \theta_2 \\ \dot{\theta}_1 \\ \dot{\theta}_2 \\ \ddot{\theta}_1 \\ \ddot{\theta}_2 \end{Bmatrix}_k = \begin{Bmatrix} \theta_1 + \Delta t \dot{\theta}_1 \\ \theta_2 + \Delta t \dot{\theta}_2 \\ \dot{\theta}_1 + \Delta t a_1/d_1 \\ \dot{\theta}_2 + \Delta t[(a_2 - L_1 \sin(\theta_2)\dot{\theta}_1^2)/d_2 - a_1(d_2 + L_1\cos(\theta_2))/d_1 d_2] \\ a_1/d_1 + \delta \\ (a_2 - L_1 \sin(\theta_2)\dot{\theta}_1^2)/d_2 - a_1(d_2 + L_1\cos(\theta_2))/d_1 d_2 + \delta \end{Bmatrix}_{k-1}. \tag{27}$$

In this test, among the three strategies proposed in Sect. 4.1, the closed-loop estimation of accelerations has been performed using the scheme based on acceleration equations with random walk (see Sect. 4.1.1). In Eq. (27), a_1 and a_2 are the accelerations measured by the two accelerometers attached to link 1 and 2, which are located at distances d_1 and d_2 from the shoulder and the elbow joints, respectively. Such accelerations are the system inputs ($\mathbf{u} = \{a_1\ a_2\}^{\mathrm{T}}$). The output vector $\mathbf{y}$ comprises the rotations of both the joints to represent correctly the zero-frequency dynamics of both the links, and therefore linearly depends on the state:

$$\mathbf{y} = \begin{Bmatrix} \theta_1 \\ \theta_2 \end{Bmatrix} = \begin{bmatrix} 1 & 0 & 0 & 0 & 0 & 0 \\ 0 & 1 & 0 & 0 & 0 & 0 \end{bmatrix} \mathbf{x}^{aug}. \tag{28}$$

This set of measurements defines a less challenging condition for the EKF since it reduces the system model nonlinearities, by making $\boldsymbol{g}$ a linear function. It is worth noticing that this choice of input and output vectors guarantees respectively the existence of $[\mathbf{S}^{\mathrm{T}}\mathbf{S}]^{-1}$ and the observability of the system for any joint configuration.

Two different tests have been carried out. The first test ("TEST 1") consists of a sequence of transient responses imposed by quasi-impulsive excitations exerted to link 1 by the actuator. The encoder and accelerometer signals recorded during the test are shown in Fig. 6. The test lasted 10 seconds. The estimated angular velocities and accelerations are shown in Figs. 7 and 8 for the shoulder and elbow joints, respectively. For sake of clarity, just the estimates obtained using the SS-UKF algorithm are shown in the figures. Nevertheless, almost

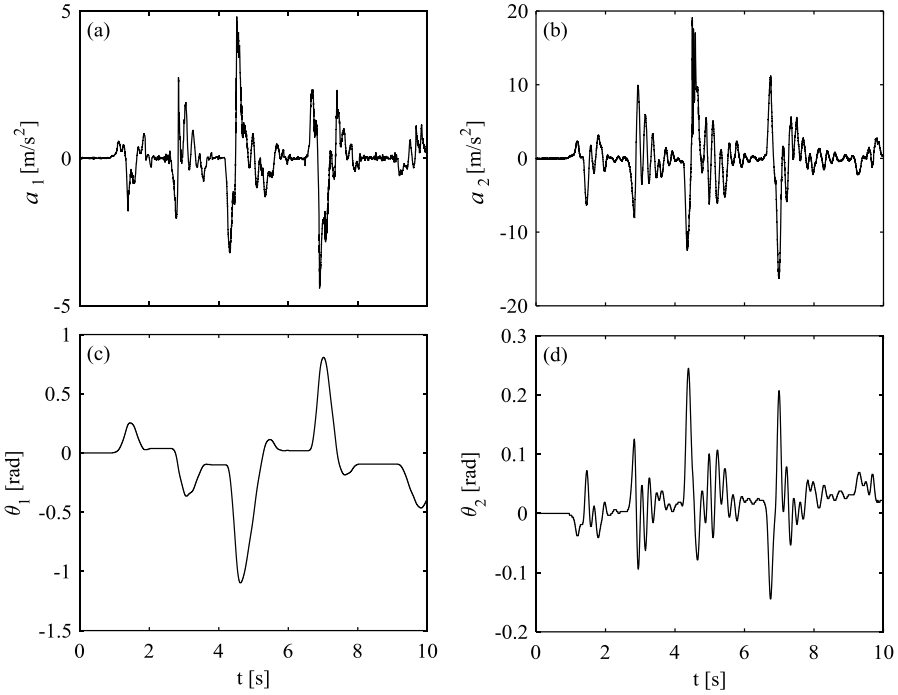

Fig. 6 TEST 1. System input: acceleration measurements at link 1 (**a**) and link 2 (**b**). System output: encoder measurements at the shoulder (**c**) and elbow (**d**) joints

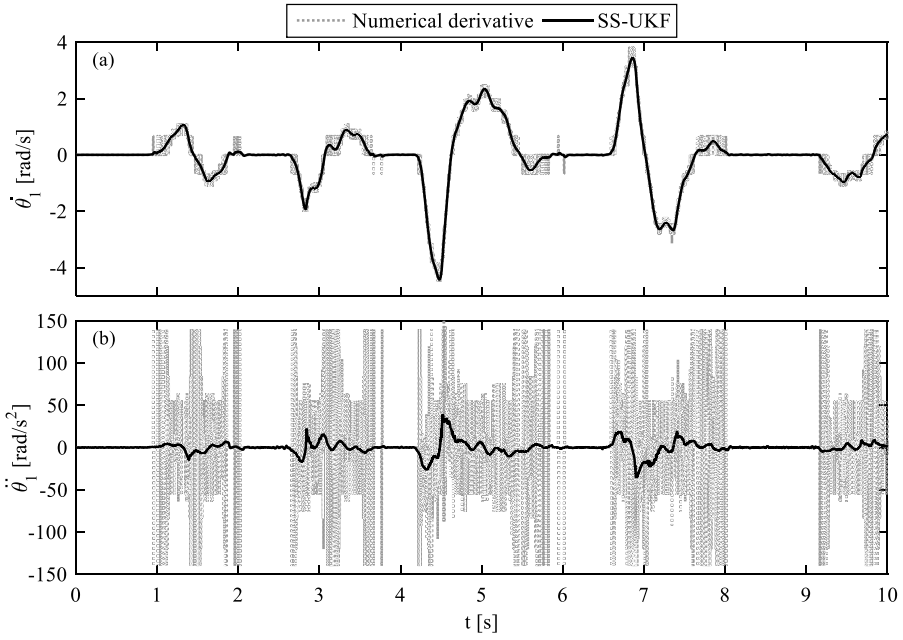

Fig. 7 TEST 1. Estimated angular velocity (**a**) and acceleration (**b**) at the shoulder joint

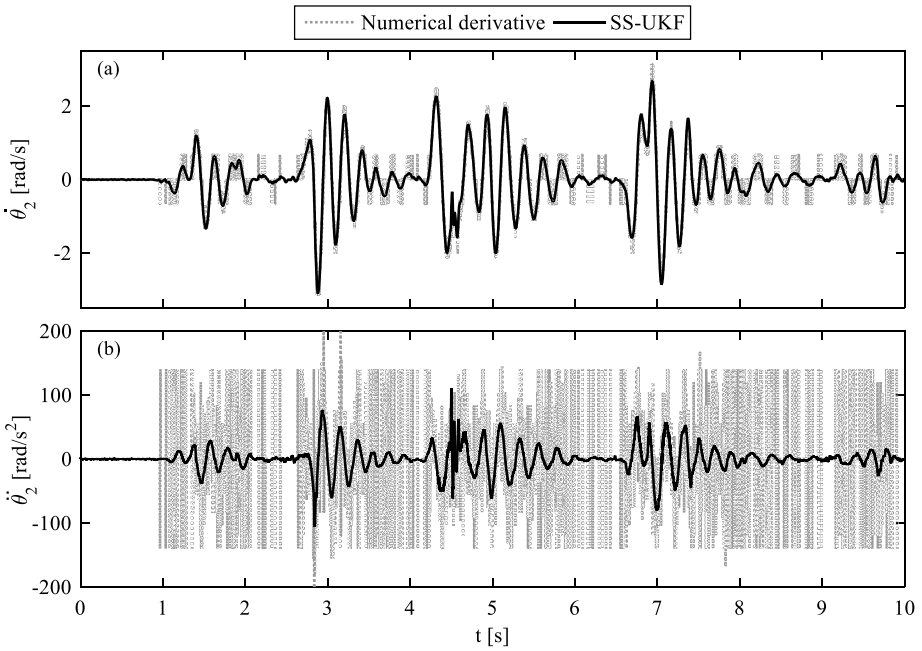

Fig. 8 TEST 1. Estimated velocity (**a**) and acceleration (**b**) at the elbow joint

identical results are obtained using the EKF algorithm. Figures 7 and 8 also show the velocities and accelerations computed by means of just numerical derivatives of encoder signals. To this purpose, a seventh-order, low-noise Lanczos differentiator [19] has been adopted, and implemented in a non-causal form (i.e. two-sided scheme), in order to smooth noise and reduce time delay. Nonetheless, the resulting velocities and accelerations appear extremely noisy. In contrast, very smooth estimations are provided by both the observers, without any significant delay. This comparison makes the usefulness of state observers apparent. The estimations provided by both the EKF and the SS-UKF, which are causal filters (in the control theory sense) and hence can operate in real-time, are much more accurate and have negligible delay. In practice, kinematic estimation grants results that might be obtained only through non-causal filtered derivatives, which, however, cannot be employed in real-time computation since they use future samples of the input and output variables.

In the second test carried out ("TEST 2"), the shoulder joint position is commanded to track a sweep excitation ranging from 10 to 1 Hz, and lasting 9 seconds. For clarity of representation, just a sample portion of each signal is shown in Figs. 9, 10, and 11. Similar results are obtained in the whole frequency range but they are not shown for brevity. The measured signals are shown in Fig. 9, while the velocities and accelerations estimated by the EKF are shown in Figs. 10 and 11. Also in this test, the EKF and the SS-UKF provide almost the same results, and hence just those obtained through the EKF are shown for clarity of representation. Once again in the same figures, velocities and accelerations obtained by means of a numerical derivative of encoder signals are shown, too.

These results are coherent with those yielded by the previous numerical investigation and corroborate the usefulness and effectiveness of the proposed approach to kinematic state estimation.

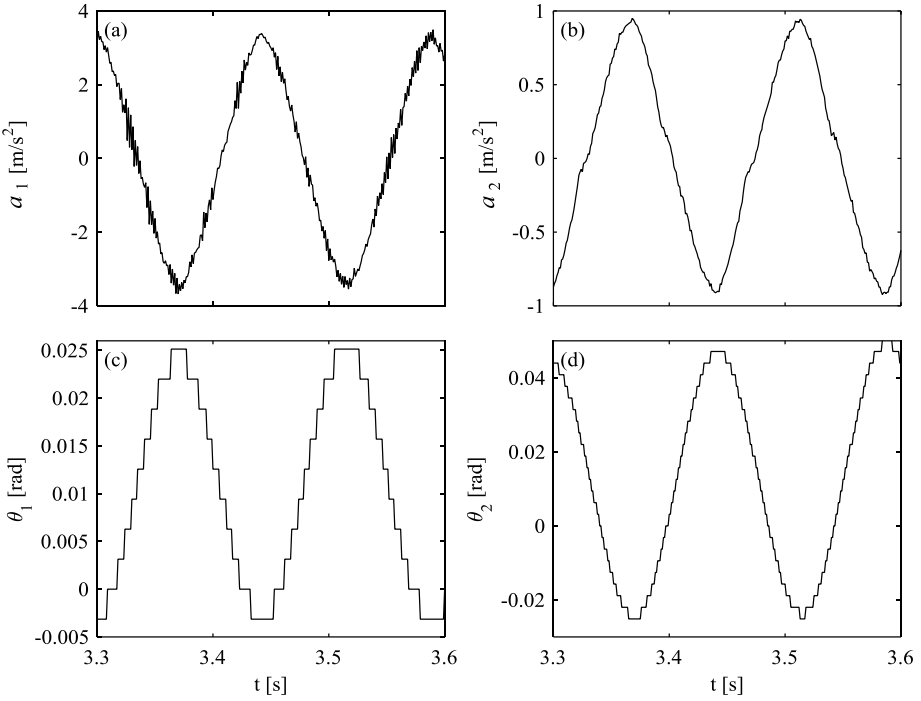

Fig. 9 TEST 2. System input: acceleration measurements at link 1 (**a**) and link 2 (**b**). System output: encoder measurements at the shoulder (**c**) and elbow (**d**) joints

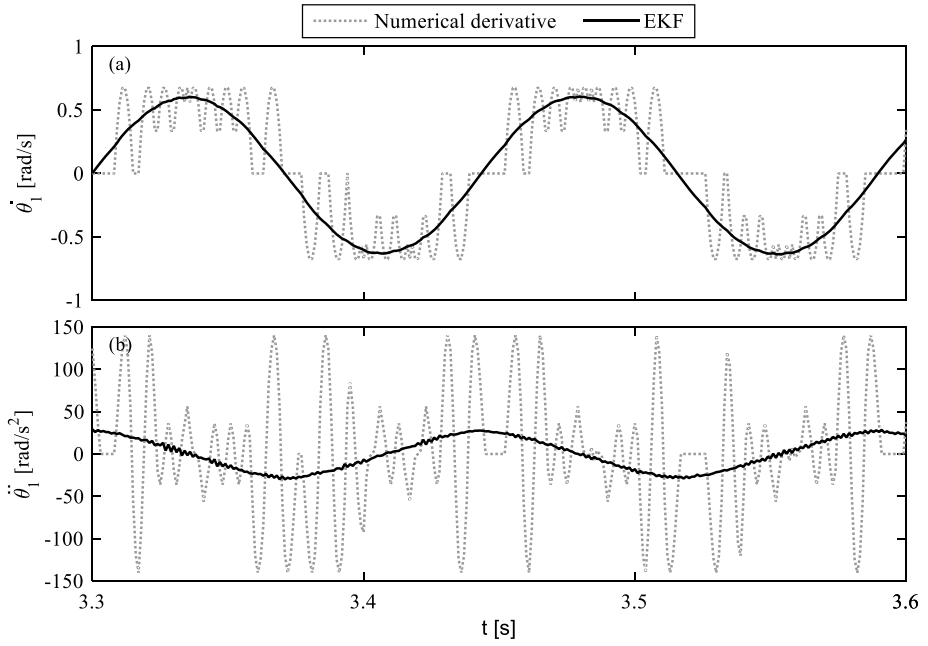

Fig. 10 TEST 2. Estimated angular velocity (**a**) and acceleration (**b**) at the shoulder joint

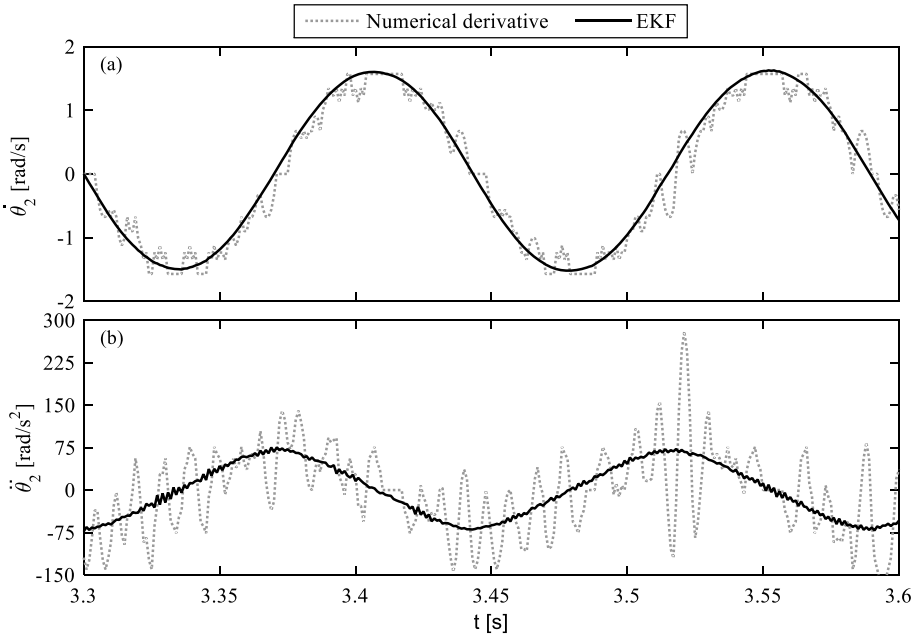

Fig. 11 TEST 2. Estimated angular velocity (**a**) and acceleration (**b**) at the elbow joint

Table 1 CPU times taken for each test

Test case		Run duration [s]	CPU time	
			SS-UKF	EKF
Slider-crank mechanism		30	8.38	12.17
Two-dof mbs	Test 1	10	0.85	1.42
	Test 2	9	0.78	1.27

5.3 CPU time comparison between filters

The computational efficiency of the proposed approach strictly depends on the algorithms used for computing both the state and the observation predictions, as well as on the features of the code implementation. Although a rigorous analysis of the computational complexity of the two observers employed goes beyond the scope of the paper, some useful indications can be found in the comparison of the computational efforts related to the two Matlab implementations of the observers.

Table 1 lists the CPU times (obtained through a PC with Core i7-2700K, RAM 16 GB, running Windows 7) required on average by each test. In all the tests, estimation has been performed offline. The CPU time of each test is much smaller than the duration of the run (i.e. of the simulation, in test case 1, and of the time interval recorded in test case 2), and hence it is expected that hard real-time can be easily achieved.

Table 1 also shows that the SS-UKF, which is renowned to be one of the most efficient among the SPKFs, ran faster than the EKF in all the tests performed. This result is a consequence of the use of numerical Jacobians in the EKF implementation proposed, rather than analytical (or symbolic) computations of these time-varying matrices. Indeed, the EKF

requires computing both the state and measurement equations and their Jacobian matrices once at each time step. In contrast, the SS-UKF requires computing both the state and measurement equations $N + 2$ times at each time step (since $N + 2$ is the number of sigma points). Given the small dimension of the state vector (N) and the simple model equations adopted, which are kinematic equations, this computation is less cumbersome than the computation of the numerical Jacobians, in the test cases proposed. Clearly, adopting analytical expressions of the Jacobians would reduce the computational effort required by the EKF, but would also increase modeling complexity since Jacobian matrices are often cumbersome to calculate in symbolic form [4] and therefore approximated formulations should be sometimes adopted [3].

6 Conclusions

This paper has introduced and presented in detail a general theory for the design of nonlinear state observers based on kinematic models, suitable for MBSs with rigid links and negligible joint clearance. The approach collects contributions from different research fields and is general, in the sense that it can be used for both open-chain and closed-chain MBSs.

The use of filters based on kinematic models is advantageous since such models are much less affected by uncertainty than the dynamic equations of motion, usually employed in state observers, and therefore the impact of model uncertainty in the estimation accuracy is considerably reduced. Indeed, kinematic state estimation just relies on geometric equations and on the measurement of kinematic quantities, while it does not require the knowledge of dynamic equations of motion and external forces, which are often unknown in real-world applications.

The paper deals with all the aspects concerning kinematic estimation, including state-space first-order formulation of the kinematic models in both continuous-time and discrete-time, and the suitable definition of system inputs and outputs. Additionally, two critical issues are tackled to extend the range of applications of kinematic filters: the estimation of the state derivative with discrete-time schemes and the estimation in model singularity. As far as the first topic is concerned, three schemes are proposed to perform closed-loop estimation of state derivative through the prediction–correction iterations, aimed at compensating the numerical derivation noise and the model uncertainty. As far as the estimation in singular configurations is concerned, a switching model is proposed, which approximates the kinematic models with a random walk model with Gaussian noise in a neighborhood of the singular configurations.

Among the numerous strategies to implement nonlinear filters based on the Kalman filter theory, particular attention is paid in this paper to the use of sigma point unscented Kalman filters (SPKFs), whose application in the field of kinematic estimation has never been proposed in literature and is here proposed for the first time. These filters are usually more accurate than the EKF in tackling nonlinearities, since they do not use model linearization to propagate the covariance matrices and therefore to compute the filter gains. Indeed, SPKFs compute the prediction of both the state vector and the covariance matrices as the weighed sum of more solutions of the constraint equations in different mechanism configurations. Besides improving the estimation accuracy, when crossing kinematic singularities, this approach does not require the time-consuming and cumbersome computation of the kinematic model Jacobian matrices.

Numerical and experimental assessment of the theory proposed is provided through two different rigid-link MBSs: a simulated closed-chain, single-dof mechanism (slider–crank

mechanism) and a laboratory test rig consisting in a two-dof, two-link, planar mechanism with two revolute joints. Estimation is performed through the EKF and, as a representative example of SPKFs, the SS-UKF. The results clearly show the correctness and the effectiveness of the theory proposed. Indeed, precise estimations of the kinematic variables are obtained, also including the derivative of the state. Model singularities are effectively crossed, too.

References

1. Caracciolo, R., Richiedei, D., Trevisani, A.: Robust piecewise-linear state observers for flexible link mechanisms. J. Dyn. Syst. Geom. Theories **130**, 031011 (2008)
2. Kalman, R.E.: A new approach to linear filtering and prediction problems. J. Basic Eng. **82**, 35–45 (1960)
3. Cuadrado, J., Dopico, D., Perez, J.A., Pastorino, R.: Automotive observers based on multibody models and the extended Kalman filter. Multibody Syst. Dyn. **27**(1), 3–19 (2012)
4. Pastorino, R., Richiedei, D., Cuadrado, J., Trevisani, A.: State estimation using multibody models and non-linear Kalman filters. Int. J. Non-Linear Mech. **53**, 83–90 (2013)
5. Jeon, S., Katou, T., Tomizuka, M.: Kinematic Kalman Filter (KKF) for robot end-effector sensing. J. Dyn. Syst. Geom. Theories **131**(2), 021010 (2009)
6. Jeon, S.: State estimation based on kinematic models considering characteristics of sensors. In: Proceedings American Control Conference, Baltimore, pp. 640–645 (2010)
7. Wang, C., Chen, W., Tomizuka, M.: Robot end-effector sensing with position sensitive detector and inertial sensors. In: Proceedings IEEE International Conference on Robotics and Automation, pp. 5252–5257 (2012)
8. Žumer, J., Slavič, J., Boltežar, M.: Minimization of the positional errors for an accurate determination of the kinematic parameters of a rigid-body system with miniature inertial sensors. Mech. Mach. Theory **81**(0), 193–208 (2014)
9. Haug, A.J.: Bayesian Estimation and Tracking: A Practical Guide. Wiley, New York (2012)
10. Van Der Merwe, R., Wan, E.A., Julier, S.: Sigma-point Kalman filters for nonlinear estimation and sensor-fusion: applications to integrated navigation. In: Proceedings of the AIAA Guidance, Navigation & Control Conference, pp. 16–19 (2004)
11. Julier, S.: The spherical simplex unscented transformation. Proc. Am. Control Conf. **3**, 2430–2434 (2003)
12. Julier, S.: The scaled unscented transformation. Proc. Am. Control Conf. **6**, 4555–4559 (2002)
13. Julier, S., Uhlmann, J.K.: Reduced sigma point filters for the propagation of means and covariances through nonlinear transformations. Proc. Am. Control Conf. **2**, 887–892 (2002)
14. De Jalón, J.G., Bayo, E.: Kinematic and Dynamic Simulation of Multibody Systems. Springer, New York (1994)
15. Grewal, M.S., Andrews, A.P.: Kalman Filtering: Theory and Practice Using MATLAB. Wiley, New York (2011)
16. Hermann, R., Krener, A.J.: Nonlinear controllability and observability. IEEE Trans. Autom. Control **22**(5), 728–740 (1977)
17. Reif, K., Günther, S., Yaz, E., Unbehauen, R.: Stochastic stability of the discrete-time extended Kalman filter. IEEE Trans. Autom. Control **44**(4), 714–728 (1999)
18. Richiedei, D., Trevisani, A.: Vibration confinement in lightly damped multibody systems: an hybrid active–passive approach. In: Proceedings ECCOMAS Thematic Conference on Multibody Dynamics, Zagreb, Croatia (2013)
19. Lanczos, C.: Applied Analysis. Courier Dover, New York (1988)